

See discussions, stats, and author profiles for this publication at: <https://www.researchgate.net/publication/222596022>

Chemical disorder and spin crossover in a mixed ethanol-2-propanol solvate of Fe(II) tris(2-picolylamine) dichloride

ARTICLE *in* NEW JOURNAL OF CHEMISTRY · JUNE 2009

Impact Factor: 3.09 · DOI: 10.1039/b823514g

CITATIONS

16

READS

32

4 AUTHORS, INCLUDING:



Dmitry Chernyshov

European Synchrotron Radiation Facility

212 PUBLICATIONS 2,123 CITATIONS

SEE PROFILE



hans-beat Buergi

University of Zurich

243 PUBLICATIONS 6,119 CITATIONS

SEE PROFILE

Chemical disorder and spin crossover in a mixed ethanol–2-propanol solvate of Fe^{II} tris(2-picolylamine) dichloride†

Dmitry Chernyshov,^{*a} Brita Vangdal,^b Karl Wilhelm Törnroos^b and Hans-Beat Bürgi^c

Received (in Montpellier, France) 5th January 2009, Accepted 3rd March 2009

First published as an Advance Article on the web 14th April 2009

DOI: 10.1039/b823514g

We compare the macroscopic and magnetic properties of three spin crossover compounds, $[\text{Fe}^{\text{II}}(2\text{-pic})_3]\text{Cl}_2 \cdot \text{EtOH}$, $[\text{Fe}^{\text{II}}(2\text{-pic})_3]\text{Cl}_2 \cdot 2\text{-PrOH}$ and $[\text{Fe}^{\text{II}}(2\text{-pic})_3]\text{Cl}_2 \cdot (\text{EtOH})_{0.744} \cdot (2\text{-PrOH})_{0.256}$ (pic = picolylamine), with their crystal structures in high-spin, low-spin and photoexcited high-spin states. We show that the spin conversion process is affected not only by the presence of solvent molecules in the crystal structure, but also by their occupational disorder in the mixed ethanol–2-propanol solvate. The solvent mixture induces a new spin crossover scenario, in which intermediate ordering of spin states is suppressed, the transition temperature is shifted and cooperativity is reduced relative to the parent, pure ethanol and 2-propanol, solvates.

Introduction

Bi-stability at the macroscopic level can arise from bi-stable molecules, from the collective behaviour of molecules, as is the case of ordinary polymorphism, or from both, as will be discussed in some detail in this paper. Complexes of Fe^{II} with ligand fields of intermediate strength may assume a low-spin (LS; $S = 0$, singlet $t_{2g}^6 e_g^0$) or high-spin (HS; $S = 2$, quintet $t_{2g}^4 e_g^2$) electronic configuration. At certain temperatures and pressures, the free energy difference between the two distinct spin isomers becomes small or close to zero. Such complexes may therefore be considered bi-stable.¹

Temperature-induced spin conversion is an entropy driven process.² On cooling, an entropically favoured HS phase is converted into an enthalpically favoured LS phase, either gradually (spin crossover) or abruptly (first-order spin transition). Sometimes intermediate phases with an ordered pattern of concurrent HS and LS species form when changing the temperature (two-step transitions).

Most molecular spin conversion solids have complex crystal structures assembled from spin-active complexes and spin-inactive counterions, solvent molecules or both. The latter components—if disordered—may show temperature-induced ordering that proceeds in parallel with spin conversion. The co-existence of ordering processes and spin conversion has been documented experimentally by diffraction experiments for compounds with disordered solvents,^{3,4} counterions^{5–7} and/or ligands.⁸

Recently, we have shown that several different alcohol solvates of $[\text{Fe}^{\text{II}}(2\text{-pic})_3]\text{Cl}_2$ (pic = picolylamine), with alcohols ranging in size from methanol to *tert*-butanol, display the same crystal architecture but different spin conversion behaviours, depending on the nature of the solvent molecules. The observed scenarios included two- and one-step transitions, continuous crossover and even complete suppression of the temperature-activated spin change.⁹ The crystal structures and physical properties of the $[\text{Fe}^{\text{II}}(2\text{-pic})_3]\text{Cl}_2$ ethanol and 2-propanol solvates as a function of temperature have been investigated in detail.^{10,11} It was found that spin conversion was accompanied by an order–disorder transition of the alcohol molecules. These observations indicate an interaction between the ordering of spin-inactive components and spin conversion. Consequently, a theory that parameterizes such couplings has been proposed for temperature-activated disorder.¹²

These findings raise questions concerning the properties of single crystals with the same overall architecture, as studied previously, but with solvent positions occupied by either one of two different solvent molecules co-crystallized deliberately from a corresponding solvent mixture. Site occupation by different solvent molecules is an example of chemical disorder that is *not* temperature dependent, because ordering would require that intact solvent molecules exchange places in the crystal, a process that is highly unlikely at room temperature and ambient pressure. Here, we describe our results for a *mixed* ethanol–2-propanol solvate of $[\text{Fe}^{\text{II}}(2\text{-pic})_3]\text{Cl}_2$, compare its crystal structure with those of its parent solvates and show how occupational disorder due to different solvent molecules modifies the spin conversion of the parent compounds containing a single type of solvent molecule.

The low temperature LS ground state of $[\text{Fe}^{\text{II}}(2\text{-pic})_3]\text{Cl}_2$ can be switched to a HS state not only by heating, but also by laser irradiation; an effect known as light-induced excited spin state trapping (LIESST).¹³ The photoswitching between LS and HS states has been recognized as a single-molecule inter-system crossing process with a quantum efficiency of ~ 1 .^{14,15}

^a Swiss Norwegian Beamlines at European Synchrotron Radiation Facility, 6 rue Jules Horowitz, BP 220, F-38043 Grenoble cedex 9, France. E-mail: dmitry.chernyshov@esrf.fr

^b Department of Chemistry, University of Bergen, 5007 Bergen, Norway

^c Department of Chemistry and Biochemistry, University of Berne, 3012 Berne, Switzerland

† Electronic Supplementary Information (ESI) available: CCDC 714607–714610. For crystallographic data in CIF or other electronic format see DOI: 10.1039/b823514g

and a dependence on cooperative interactions. LIESST leads to the formation of a photoinduced macroscopic phase. The photoswitching between the macroscopic LS and HS phases shows characteristics of non-adiabatic collective phenomena, *e.g.* a threshold laser intensity, an incubation time and the formation of spin-like domains, all of them as expected for a photoinduced phase transition (PIPT).^{16,17} PIPTs at low temperatures are of basic interest as they may give access to new phases that are normally hidden under thermal equilibria, but become accessible as the influence of thermal fluctuations is minimized.^{18,19} Here, we compare the crystal structure of the HS phase of the mixed ethanol–2-propanol solvate of $[\text{Fe}^{\text{II}}(2\text{-pic})_3]\text{Cl}_2$ at 200 K with its photoinduced HS phase at 16 K, and especially their chemically and thermally-induced structural disorder.

Results

Temperature-induced phases

Four diffraction data sets have been collected for $[\text{Fe}^{\text{II}}(2\text{-pic})_3]\text{Cl}_2 \cdot (\text{EtOH})_{0.744} \cdot (2\text{-PrOH})_{0.256}$ at 200, 118 and 16 K, and under laser irradiation at 16 K; all of a quality suitable for analysing structural disorder (Table 1).[†]

At all temperatures, the structures consist of layers of hydrogen-bonded $[\text{Fe}^{\text{II}}(2\text{-pic})_3]\text{Cl}_2$ complexes (Fig. 1) and chloride ions, closely similar to those found in their pure ethanol and 2-propanol solvent analogues. The hydrophilic OH groups of the alcohol molecules are attached to the chloride ions *via* hydrogen bonds, while their hydrocarbon moieties nestle into the cavities formed by pairs of pyridine rings of the $[\text{Fe}^{\text{II}}(2\text{-pic})_3]^{2+}$ ions from a neighboring layer, thereby linking the hydrophilic layers into a 3D crystal structure through hydrophobic contacts.^{10,11}

The molecular structures of the $[\text{Fe}^{\text{II}}(2\text{-pic})_3]^{2+}$ fragment for the ethanol, 2-propanol and mixed ethanol–2-propanol solvates in their HS states are compared in Fig. 2. A least-squares superposition of the respective FeN_6 fragments indicate a close similarity between the molecular structures of all three compounds at high temperature (HT; 200 K), suggesting similar ligand fields and thus similar spin-crossover temperatures.

Occupation factors of the solvent molecules were refined with the low temperature (16 K; LT) data, which showed all the $[\text{Fe}^{\text{II}}(2\text{-pic})_3]\text{Cl}_2$ complexes to be in the LS state. The ethanol and 2-propanol occupation coefficients of 0.744(6) and 0.256(6), respectively, were kept fixed in the refinements of the other three data sets. Although intrinsically occupationally disordered, each of the two different solvent molecules

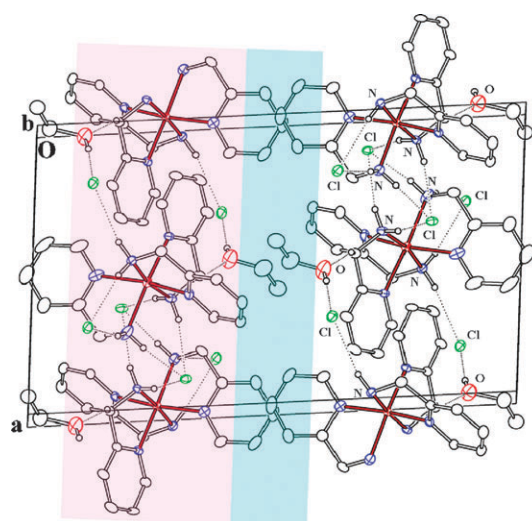


Fig. 1 Crystal packing features of $[\text{Fe}^{\text{II}}(2\text{-pic})_3]\text{Cl}_2 \cdot (\text{EtOH})_{0.744} \cdot (2\text{-PrOH})_{0.256}$. The hydrophilic hydrogen bond (dashed lines) layer is shaded in pink and the hydrophobic layer in turquoise. The donor and acceptor elements are identified on the right-hand side.

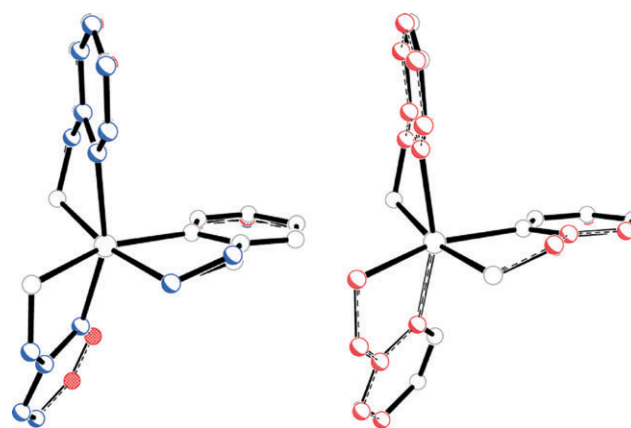


Fig. 2 Least-squares superpositions of FeN_6 fragments. Left: the $[\text{Fe}^{\text{II}}(2\text{-pic})_3]^{2+}$ fragments of the ethanol, 2-propanol and mixed solvates in their HT/HS phases (200 K). Atom colour code: mixed solvate—blue (shaded circles), 2-propanol—red (hatched circles, r.m.s. deviation 0.0222 Å), ethanol—black (open circles r.m.s. deviation 0.0105 Å). Right: the $[\text{Fe}^{\text{II}}(2\text{-pic})_3]^{2+}$ fragments in the HT/HS phase (200 K—red, shaded circles) and LT/HS phase (16 K under laser light—black, open circles); r.m.s. distance = 0.008 Å.

is found in a single position (and orientation) at 16 K. At 118 and 200 K, both kinds of solvent molecules are found to be disordered over two positions. Unit cell dimensions, average

Table 1 Summary of the X-ray experimental data for four data sets of the mixed solvate $[\text{Fe}^{\text{II}}(2\text{-pic})_3]\text{Cl}_2 \cdot (\text{EtOH})_{0.744} \cdot (2\text{-PrOH})_{0.256}$

	16 K LT/LS	16 K LT/HS laser ^a	118 K 40 : 60 HS : LS	200 K HT/HS
Reflections integrated	13 843	13 603	15 797	16 277
θ_{min} to θ_{max} (°)	2.84 to 25.45	2.81 to 25.45	2.82 to 25.43	2.79 to 25.45
Unique reflections	4295	4386	4374	4519
R_{int}	0.0298	0.0335	0.0279	0.0280
R_1	0.0291	0.0319	0.0312	0.0309
wR_2	0.0697	0.0828	0.0739	0.0714

^a Measured under laser irradiation, $\lambda = 632.8$ nm, and a 5 mW maximum output.

Table 2 Unit cell dimensions, bond lengths, and solvent disorder for the HS and LS phases of ethanol, 2-propanol and mixed solvates. The non-standard space group setting $B2_1/c$ was chosen for easier comparison with related solvates.^{10,11} The first row in the solvent disorder section shows the occupation factor of the ethanol and the second of the 2-propanol molecule. Values separated by “/” indicate positional disorder, which is absent at 16 K

		Ethanol	Mixture	2-Propanol
HT/HS 200 K	$a/\text{\AA}$	11.4725(6)	11.4808(8)	11.5302(4)
	$b/\text{\AA}$	21.9166(12)	21.9300(12)	22.0163(8)
	$c/\text{\AA}$	19.4189(10)	19.6473(11)	20.1391(9)
	β (°)	94.041(4)	94.923(5)	96.027(1)
	$d(\text{Fe-N})/\text{\AA}$	2.192(1)	2.192(2)	2.197(2)
	Solvent disorder	0.832(5)/0.168	0.478(9)/0.262	—
LT/LS 16 K	$a/\text{\AA}$	—	0.139(3)/0.121	0.69(1)/0.31
	$b/\text{\AA}$	11.3256(7)	11.3341(12)	11.3568(13)
	$c/\text{\AA}$	21.5132(15)	21.512(2)	21.5733(16)
	β (°)	19.1574(9)	19.3534(18)	20.1225(24)
	$d(\text{Fe-N})/\text{\AA}$	94.589(7)	95.525(8)	104.968(13)
	Solvent disorder	2.012(1)	2.010(2)	2.001(3)
		1	0.744(6)	—
		—	0.256(6)	1

iron–ligand bond lengths, and solvent disorders for the HS and LS phases of the ethanol, 2-propanol and mixed solvates are summarized in Table 2.

At 200 K, $[\text{Fe}^{\text{II}}(2\text{-pic})_3]^{2+}$ is in the HS state, as seen from the $\langle\text{Fe-N}\rangle$ bond length. This average distance is 0.182 Å longer than that in the LS state at 16 K, a difference similar to those found in other solvates.⁹ At 118 K, only ~40% of the spin-active centres are in the HS state, implying that the nitrogen ligand atoms are disordered over two positions about 0.18 Å apart, too close to be resolved with X-ray diffraction data. The disorder is modelled in terms of average nitrogen positions associated with atomic displacement parameters (ADPs) containing a contribution reflecting the disorder. This contribution can be extracted from a comparison of the ADPs of the Fe and N atoms at the three different temperatures. Differences in ADPs along the internuclear N–Fe vectors $\langle\Delta U_{\text{Fe-N}}\rangle = \langle r_{\text{N-Fe}}^T \{U(\text{N}) - U(\text{Fe})\} r_{\text{N-Fe}} \rangle$ are given in Table 3 (Hirshfeld differences). They are small at high and low temperatures, where all complexes are in the same spin state, the non-zero values being due to Fe–N stretching motions. They are more than twice as large at intermediate temperatures, indicative of disorder. The value of 0.011(1) Å² agrees with the estimate $(0.18/2)^2 + 0.004 = 0.012$ Å², where the first term accounts for the nitrogen disorder and the second term for the Fe–N stretching motion, as in the ordered phases. It also agrees with previous findings.²⁰

Fig. 3 shows transition curves of all three solvates in terms of fractions of HS molecules as a function of temperature. The HS fractions were obtained from magnetisation measurements. The transition curve of the mixed solvate (middle) is gradual without hysteresis, different to those of the pure solvates, both of which show 1st order transitions. There are also notable differences in the transition temperatures, 118 K for the ethanol solvate, 122 K for the mixed solvate and 147 K

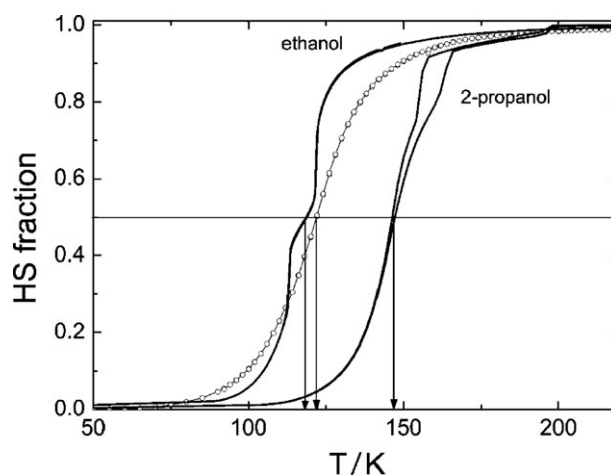


Fig. 3 The fraction of HS states as a function of temperature (transition curves) for the ethanol,¹⁰ 2-propanol¹¹ and mixed (middle, open circles) solvates, all obtained from SQUID data. The arrows show the corresponding transition temperatures, $T_{1/2}$.

for the 2-propanol solvate. Given the similarity of the three crystal structures, the differences in the spin transition curves shown in Fig. 2 are contrary to expectations and require further discussion.

Light-induced low temperature high-spin phase

Laser irradiation at 16 K resulted in a structure with increased unit cell dimensions and an $\langle\text{Fe-N}\rangle$ bond length corresponding to a low temperature high-spin phase (LT/HS). The geometry of the $[\text{Fe}^{\text{II}}(2\text{-pic})_3]^{2+}$ cation (Fig. 2) and Hirshfeld differences were very similar to those of the HT/HS phase (Table 3). In contrast to the HT/HS phase,

Table 3 Isotropically-averaged ADPs and Hirshfeld differences for the mixed solvate at three temperatures

ADP/Å ²	HT/HS (200 K)	40 : 60 HS : LS (118 K)	LT/LS (16 K)	LT/HS (16 K) laser
$U_{\text{iso}}(\text{Fe})$	0.02317(8)	0.01478(9)	0.00401(8)	0.0064(1)
$\langle U_{\text{iso}}(\text{N}) \rangle$	0.0288(4)	0.0226(5)	0.0067(3)	0.0091(4)
$\langle\Delta U_{\text{Fe-N}}\rangle$	0.0038(8)	0.0111(11)	0.0043(8)	0.004(1)

the solvent molecules in the LT/HS phase are ordered, as in the LT/LS phase.

Discussion and conclusions

Temperature-induced spin crossover

The crystal symmetry, the general crystal architecture, *i.e.* the packing of the anions, cations and solvent molecules, and the structural details of the $[\text{Fe}^{\text{II}}(2\text{-pic})_3]\text{Cl}_2$ complexes are very similar for the three solvates (Fig. 2). The solvent molecules in all three solvates show positional disorder in the HS state. In the LS state, the ethanol and 2-propanol molecules in all solvates assume positional order—although they maintain, of course, occupational disorder in the mixed solvate.

The spin transition curves of the three solvates are distinctly different (Fig. 3). The curve of the ethanol solvate shows a plateau centred close to a HS fraction of ~ 0.5 , *i.e.* at $T_{1/2} = 118$ K. The corresponding curve of the 2-propanol solvate has a plateau at a HS fraction of ~ 0.95 between ~ 160 and ~ 190 K. In both cases, the plateau is bracketed by first-order transitions delimiting intermediate phases, in which the orientations of the solvent molecules, the HS and the LS complexes are (partially) ordered and no longer distributed randomly throughout the crystal lattice.^{10,11} At high temperatures all spin-active molecules are in their HS state, and the solvent molecules are disordered. At low temperatures, all spin-active molecules are in their LS state, and the solvent molecules are ordered.

The transition curve of the mixed solvate is continuous, without plateaus or first-order transitions, implying that the formation of intermediate phases with ordered distributions of HS and LS states is completely suppressed by the chemical disorder of the two different kinds of solvent molecules. Its $T_{1/2}$ is 122 K, closer to that of the ethanol solvate, in agreement with the large ethanol content of $\sim 75\%$. However, the transition curve is not a weighted average of those of the parent solvates. Above ~ 115 K, it runs between the curves of the pure solvates. Below this temperature, it runs ahead of the two pure solvates.

The diffraction data do not show splitting, broadening of the Bragg reflections, any change in space group symmetry or diffuse scattering, all of which could indicate macroscopic phase separation, or mesoscopic correlations and de-mixing of HS and LS molecules. Taken together, these facts imply that the deliberate mixing of two different solvent molecules within a single crystal lattice has resulted in a new spin crossover scenario, where the positional order–disorder process of the solvent molecules is preserved, the intermediate ordering of spin states is suppressed, the transition temperature is shifted, and cooperativity is reduced relative to the parent compounds.

The observations described here for a mixed solvate show that replacing one out of four ethanol molecules with 2-propanol (differing from ethanol only by a methyl group) affects the spin crossover of the $[\text{Fe}^{\text{II}}(2\text{-pic})_3]\text{Cl}_2$ complexes compared to those of the pure solvates, but maintains its coupling with the ordering process of the spin-inactive alcohol molecules. Presumably, the coupling is mediated by weak but

numerous van der Waals contacts between the pyridine ligands of the $[\text{Fe}^{\text{II}}(2\text{-pic})_3]\text{Cl}_2$ complex and the hydrocarbon parts of the solvent molecules. The present results, taken together with earlier observations on several pure solvates, indicate that subtle changes in van der Waals interactions modify the couplings sufficiently to alter the spin crossover behaviour, and are therefore at least as important as small changes in the coordination geometry at the Fe^{II} centre and thus of the ligand field.^{9–11}

Light-induced spin crossover

Photoexcitation at 16 K leads to a LT/HS phase whose arrangement of the $[\text{Fe}^{\text{II}}(2\text{-pic})_3]^{2+}$ cations and Cl^- anions is very closely similar to that seen in the HT/HS structure. There is only a minor change, by as little as $\sim 3^\circ$, in the dihedral angle between the two pyridine rings forming the cleft that hosts the alcohol molecules (Fig. 1). The difference in the solvent sublattice is more severe: the solvent molecules, while being intrinsically occupationally-disordered in both phases, are positionally-ordered in the LT/HS phase but disordered in the HT/HS phase.

A similar behaviour was observed for $[\text{FeL}_2](\text{BF}_4)_2$ ($\text{L} = 2,6\text{-di}(\text{pyrazol-1-yl})\text{pyridine}$), where the BF_4^- anion was disordered in the HT/HS state but ordered in both the LT/LS and photoinduced LT/HS phases.²¹

The photoexcited LT/HS form of the ethanol solvate has been studied by several techniques to probe its structure and dynamics. Raman scattering experiments on the LT/HS phase reportedly show new symmetry-forbidden vibrational modes and a more complex pattern than that for the HT/HS phase.²² These findings have been interpreted in terms of a cooperative Jahn–Teller deformation of the $[\text{Fe}^{\text{II}}(2\text{-pic})_3]^{2+}$ cations, leading to a loss of crystalline inversion symmetry in the photoexcited phase.²² A displacement of the carbon atoms, corresponding to a N–C–C bending mode in the aminomethyl side chain of the picolylamine ligand, has also been suggested as a possible explanation for the symmetry lowering.²³

Long-range correlation of either deformation would lower the diffraction symmetry. In the case of our mixed solvate in its LT/HS phase, no change of crystal symmetry has been observed: with neither the appearance of additional Bragg reflections, indicating the appearance of superstructure reflections, nor the disappearance of systematic absences due to the disappearance of the 2_1 -axis or the c -glide. Uncorrelated distortions would preserve an average $P2_1/c$ symmetry but would affect the atomic displacement parameters of the nitrogen atom and the carbon atoms involved in the N–C–C bending. No significant effect on the ADPs of the nitrogen and carbon atoms could be discerned in the LT/HS phase of the mixed solvate. Our observations agree closely with those of XAFS experiments and previous diffraction studies on the photoexcited form of the ethanol solvate, which also indicate very similar structures of the $[\text{Fe}^{\text{II}}(2\text{-pic})_3]$ complex in its HT/HS and LT/HS forms.^{24,25}

Photoexcitation of the mixed solvate results in a new structural HS state, unchanged with respect to the architecture formed by the spin-active $[\text{Fe}^{\text{II}}(2\text{-pic})_3]\text{Cl}_2$ complexes but

different with respect to the solvent sublattice. This state is not accessible by temperature activation.

General remarks

Nowadays, transition curves for spin crossover compounds are easily and routinely derived from macroscopic properties, such as colour or magnetisation. It is tempting to interpret these properties in structural terms or to correlate them with structural data from a diffraction experiment of limited resolution collected at a single temperature. Such interpretations are necessarily limited, and it is well worthwhile searching for weak superstructure reflections with the help of area detectors and reconstructions of reciprocal space. Good quality, high resolution diffraction data as a function of temperature are necessary to reveal the finer details of spin conversion, which may include order/disorder processes, not only of spin active complexes, but also of spin-inactive solvents or counterions, as well as various couplings between these processes. Experimental effort and detail is essential if a realistic picture of the spin conversion process is to be uncovered, a picture that is not necessarily visible by the measurement of macroscopic properties alone.

Experimental

The complex was prepared according to a published method.²⁶ FeCl₂·4H₂O (0.55 g, 2.77 mmol) was dissolved in the minimum amount of a 1 : 1 mixture of ethanol and 2-propanol. 3.3 equivalents of the ligand were added slowly, and the solution was left stirring for 2 h at ~60 °C. The solution was then slowly cooled without stirring and left standing so that the excess solvent could evaporate. The resulting crystals were washed in a 1 : 1 mixture of acetone and dichloromethane. The reactants and product were handled in an oxygen-free atmosphere.

The X-ray diffraction data of the mixed ethanol–2-propanol solvate were collected on the SNBL beamline BM1A at the ESRF synchrotron in Grenoble (France) with a MAR345 image-plate area detector using $\lambda = 0.71058$ Å, φ -scans of 2° and a readout pixel resolution of 150 µm. The sample was cooled with an Oxford Cryostream series 600 N₂ cryostat, and two data sets covering 360° in φ were collected at 200 K (HT/HS state) and 118 K (~40 : 60 HS : LS ratio), respectively. An Oxford Diffraction HelixJet cryo-cooler was used to cool the sample down to 16 K at which temperature two more data sets were collected, first without laser irradiation (LT/LS state) and then under laser light from a helium–neon laser with $\lambda = 632.8$ nm and a 5 mW maximum output (LT/HS).

Intensities were integrated with CrysAlis,²⁷ and reflections shadowed by the coolers were removed from the data by means of locally written software. A set of layers in reciprocal space were reconstructed with the help of CrysAlis in order to check for possible superstructure reflections or diffuse scattering. Empirical absorption corrections and the scaling of integrated intensities were undertaken using SADABS software.²⁸

The crystal structures were solved with SHELXS and refined with SHELXL.²⁹ Hydrogen atoms were input as riding

atoms, with their isotropic displacement parameters fixed at 1.2U_{eq}(CH, CH₂) and 1.5U_{eq}(CH₃, OH) of their respective parent atoms.

Magnetic susceptibility measurements between 2 and 298 K were performed using a SQUID MPMS-XL5 (Quantum Design) instrument on a freshly made microcrystalline sample in a field-cooling mode (field: 1000 Oe). The susceptibilities measured from samples were corrected for diamagnetic contributions of the sample holder, normalized to 1 mol of sample and then corrected for the diamagnetic contribution of the sample itself. The HS fraction as a function of temperature, $\gamma_{\text{HS}}(T)$, was calculated from the susceptibilities $\chi_{\text{HT}}(T)$ and $\chi_{\text{LT}}(T)$, where $\chi(T) = \gamma_{\text{HS}}(T)\chi_{\text{HT}}(T) + \chi_{\text{LT}}(T)$.

Acknowledgements

We thank the staff of the Swiss Norwegian Beam Lines for their continuous support.

References

- 1 F. Varret, A. Bleuzen, K. Boukheddaden, A. Bousseksou, E. Codjovi, C. Enachescu, A. Goujon, J. Linares, N. Menendez and M. Verdaguer, *Pure Appl. Chem.*, 2002, **74**(11), 2159.
- 2 P. Gülich and H. A. Goodwin, *Top. Curr. Chem.*, 2004, **233**, 1.
- 3 E. König, G. Ritter, S. K. Kulshreshtha, J. Waigel and L. Sacconi, *Inorg. Chem.*, 1984, **23**, 1241.
- 4 C.-C. Wu, J. Jung, P. K. Gantzel, P. Gülich and D. N. Hendrickson, *Inorg. Chem.*, 1997, **36**, 5339.
- 5 E. König, G. Ritter, S. K. Kulshreshtha and S. M. Nelson, *Inorg. Chem.*, 1982, **21**, 3022.
- 6 J. M. Holland, J. A. McAllister, Z. Lu, C. A. Kilner, M. Thornton-Pett and M. A. Halcrow, *Chem. Commun.*, 2001, 577.
- 7 V. A. Money, J. Elhaik, I. R. Evans, M. A. Halcrow and J. A. K. Howard, *Dalton Trans.*, 2004, **1**, 65.
- 8 G. S. Matouzenko, A. Bousseksou, S. A. Borshch, M. Perrin, S. Zein, L. Salmon, G. Molnar and S. Lecocq, *Inorg. Chem.*, 2004, **43**, 227.
- 9 M. Hostettler, K. W. Törnroos, D. Chernyshov, B. Vangdal and H.-B. Bürgi, *Angew. Chem.*, 2004, **116**, 4689 (*Angew. Chem., Int. Ed.*, 2004, **43**, 4589).
- 10 D. Chernyshov, M. Hostettler, K. W. Törnroos and H.-B. Bürgi, *Angew. Chem.*, 2003, **115**, 3955 (*Angew. Chem., Int. Ed.*, 2003, **42**, 3825).
- 11 K. W. Törnroos, M. Hostettler, D. Chernyshov, B. Vangdal and H.-B. Bürgi, *Chem.-Eur. J.*, 2006, **12**(24), 6207.
- 12 D. Chernyshov, N. Klinduhov, K. W. Törnroos, M. Hostettler, B. Vangdal and H.-B. Bürgi, *Phys. Rev. B: Condens. Matter Mater. Phys.*, 2007, **76**, 014406.
- 13 S. Decurtins, P. Gülich, K. M. Hasselbach, A. Hauser and H. Spiering, *Inorg. Chem.*, 1985, **24**, 2174.
- 14 C. Enachescu, U. Oetliker and A. Hauser, *J. Phys. Chem. B*, 2002, **106**, 9540.
- 15 A. Hauser, *Top. Curr. Chem.*, 2004, **234**, 155.
- 16 Y. Morimoto, M. Kamiya, N. Nakamura, A. Nakamoto and N. Kojima, *Phys. Rev. B: Condens. Matter Mater. Phys.*, 2006, **73**, 012103.
- 17 K. Ichiiyanagi, J. Hebert, L. Toupet, H. Cailleau, P. Guionneau, J.-F. Létard and E. Collet, *Phys. Rev. B: Condens. Matter Mater. Phys.*, 2006, **73**, 060408.
- 18 T. Ogawa, *Phase Transitions*, 2002, **75**(7–8), 673.
- 19 P. Huai and T. Nasu, *Phase Transitions*, 2002, **75**(7–8), 649.
- 20 K. Chandrasekhar and H. B. Bürgi, *Acta Crystallogr., Sect. B: Struct. Sci.*, 1984, **40**, 387.
- 21 V. A. Money, I. R. Evans, M. A. Halcrow, A. E. Goeta and J. A. K. Howard, *Chem. Commun.*, 2003, 158.
- 22 T. Tayagaki and K. Tanaka, *Phys. Rev. Lett.*, 2001, **86**, 2886.
- 23 T. Tayagaki, K. Tanaka and H. Okamura, *Phys. Rev. B: Condens. Matter Mater. Phys.*, 2004, **69**, 064104.

-
- 24 H. Oyanagi, T. Tayagaki and K. Tanaka, *J. Lumin.*, 2006, **119–120**, 361.
- 25 N. Huby, L. Guérin, E. Collet, L. Toupet, J.-C. Ameline, H. Cailleau, T. Roisnel, T. Tayagaki and K. Tanaka, *Phys. Rev. B: Condens. Matter Mater. Phys.*, 2004, **69**, 020101.
- 26 M. Sorai, J. Ensling and P. Gülich, *Chem. Phys.*, 1976, **18**, 199.
- 27 *CrysAlis (Version 1.171.31.4)*, Oxford Diffraction Ltd., Oxford, UK, 2006.
- 28 G. M. Sheldrick, *SADABS (Version 2.06)*, University of Göttingen, Göttingen, Germany, 2002.
- 29 G. M. Sheldrick, *Acta Crystallogr., Sect. A: Fundam. Crystallogr.*, 2008, **64**, 112.